PHYSICAL REVIEW B VOLUME 27, NUMBER 9 1 MAY 1983

Positron annihilation on pure and carbon-doped α-iron in thermal equilibrium

L. De Schepper
Materials Physics Group, Limburgs Universitair Centrum, B-3610 Diepenbeek, Belgium

D. Segers, L. Dorikens-Vanpraet, and M. Dorikens
Instituut voor Nucleaire Wetenschappen, Rijksuniversiteit te Gent, Proeftuinstraat 42, B-9000 Gent, Belgium

G. Knuyt and L. M. Stals
Materials Physics Group, Limburgs Universitair Centrum, B-3610 Diepenbeek, Belgium

P. Moser
Section de Physique du Solide Département de Recherche Fondamentale, Centre d'Etudes Nucléaires de Grenoble, Boîte Postale 85X, F-38041 Grenoble Cedex, France
(Received 8 November 1982)

Positron-annihilation S-parameter measurements in thermal equilibrium on pure and carbon-doped (50 and 750 at. ppm) α-iron are presented. It is shown that trapping of positrons in both monovacancies and carbon-vacancy pairs occurs, even far above the dissociation temperature of the vacancy pairs. Therefore, a three-state trapping model is used in the analysis of the measured S curves. The vacancy-formation enthalpy in both the paramagnetic and ferromagnetic state is deduced: It is found to be 1.79 ± 0.10 eV in the paramagnetic state and 2.0 ± 0.2 eV in the ferromagnetic state. These values are larger than those published so far. The activation enthalpy for vacancy migration obtained by combining the values cited above with recently published self-diffusion enthalpy values confirms the applicability of the one-interstitial model in α-iron.

I. INTRODUCTION

The values of the vacancy-migration enthalpy in α-iron has been the subject of a long-standing controversy. The value of 0.55 eV, corresponding to free migration of the monovacancy in recovery stage III (200–230 K), has been put forward in the so-called one-interstitial model.[1] On the other hand, it has also been suggested that a second type of self-interstitial atom would migrate freely in stage III and that the free migration of the vacancy would occur at higher temperatures, i.e., in stage IV [480–540 K (Ref. 2)]; in this so-called two-interstitial model the vacancy-migration enthalpy is about 1.3 eV. The controversy on a choice between the two models has recently been reviewed.[3]

In the last few years more and more experiments have been interpreted in favor of the one-interstitial model. Particularly positron lifetime measurements on pure and carbon-doped iron after irradiation at low temperature have given serious evidence for vacancy migration in stage III.[4–7] Although some authors have criticized this interpretation,[8] it is clear that it is very hard to explain these measurements in terms of the two-interstitial model.[9,10] Further strong evidence for vacancy migration in stage III has been given by very recent studies of the vacancy mobility in extremely pure iron under irradiation in a high-voltage electron microscope.[11–14]

The main remaining argument against the one-interstitial model is the fact that the ferromagnetic vacancy-migration enthalpy that can be deduced by subtracting the vacancy-formation enthalpy from the self-diffusion enthalpy is about equal to the activation enthalpy for free migration of a defect in the stage-IV range.[15–17] Indeed, values of the vacancy-formation enthalpy in the ferromagnetic state reported in the past vary between 1.4 and 1.6 eV (see Table I), while the originally reported value for the self-diffusion enthalpy in this state is 2.99 eV.[18] However, a recent analysis of existing self-diffusion data by some of the present authors yielded a considerably lower value for the self-diffusion enthalpy in ferromagnetic iron.[19] It has also been suggested that the literature values of the vacancy-formation enthalpy cited above could be influenced

TABLE I. Values for the vacancy-formation enthalpy in iron (in eV).

α and δ phase				
Ferromagnetic	Paramagnetic	γ phase	Method[a]	Reference
1.5±0.1	1.5±0.1	1.5±0.1	*W*	25
1.60±0.15[b]	1.53±0.15	1.54±0.15	*W*	15
1.4±0.1	1.40±0.10	1.7±0.2	NPC	24
	1.60±0.10	1.40±0.15	NPC	23
2.0±0.2	1.79±0.10		*S*	this work

[a]NPC is the normalized peak counting rate in angular correlation, *W* is the Wing parameter in Doppler broadening, *S* is the *S* parameter in Doppler broadening.
[b]Theoretical extrapolation based on the paramagnetic value.

by the strong interaction between vacancies and residual carbon atoms in the sample.[20] It is indeed well known that the dissociation enthalpy of the carbon-vacancy pair in α-iron is high, i.e., between 1.4 and 1.6 eV (Refs. 5, 7, and 21); this corresponds to a binding energy of about 1.0 eV if the vacancy-migration enthalpy of the one-interstitial model is applied. Calculations have shown that this strong interaction between interstitial carbon atoms and vacancies can lead to a substantial thermodynamical concentration of carbon-vacancy pairs (in equilibrium with single vacancies), even far above the dissociation temperature of the pair.[20] This idea has been confirmed by a recent void-swelling experiment on iron irradiated with carbon ions.[22] It is very likely that these carbon-vacancy pairs would influence the determination of the vacancy-formation enthalpy by the positron method since, at least at ambient temperatures, it has been established that they are nearly as effective in trapping positions as monovacancies and that the positron lifetime in the pair is nearly equal to that in a single vacancy.[4,5]

In search of an effect of carbon-vacancy pairs, we performed positron annihilation measurements in thermal equilibrium using the Doppler-broadening technique. We present in this paper *S*-parameter measurements between $\sim$600 and 1183 K (the $\alpha \rightarrow \gamma$ transition temperature) on three iron samples: extremely pure iron (analysis is given in Table II), iron doped with 50 at. ppm carbon, and iron doped with 750 at. ppm carbon. It will be shown that differences between the *S* curves of these samples in the temperature range where positron trapping in defects occurs should be attributed to carbon-vacancy pairs.

The analysis of the *S* curve for pure iron will only give information on the vacancy-formation enthalpy in the paramagnetic state, since no noticeable trapping of positrons is observed below the Curie temperature (1043 K). This is in agreement with the viewpoint of Matter *et al.*[23] and Schaefer *et al.*[15]; the first group of authors gave no value for the vacancy-formation enthalpy in the ferromagnetic state, while the value given by the second group is only an estimated value (see Table I). On the other hand, Kim and Buyers[24] and Maier *et al.*[25] assumed the vacancy-formation enthalpy to be equal in the ferromagnetic and paramagnetic states; therefore, only one value was given for both states (see Table I). The argument for justifying this assumption was that no discontinuity in the *S* curve was observed at the Curie point.[24] However, it will be shown in Sec. III that, if ferromagnetic ordering is properly taken into account, this absence of a discontinuity does not

TABLE II. Chemical analysis of the very pure iron sample. Residual concentrations are given in at. ppm.

Element	Residual concentration	Element	Residual concentration	Element	Residual concentration
$_{1}$H	<1	$_{12}$Mg	0.2	$_{27}$Co	≤ 0.1
^{3}Li	<0.025	$_{13}$Al	1	$_{28}$Ni	0.1
$_{4}$Be	<0.025	$_{14}$Si	20	$_{29}$Cu	≤ 0.15
$_{5}$B	<0.08	$_{15}$P	0.02	$_{30}$Zn	≤ 0.1
$_{6}$C	≤ 1	$_{16}$S	0.4	$_{40}$Zr	≤ 0.05
$_{7}$N	≤ 0.2	$_{22}$Ti	0.2	$_{41}$Nb	<0.1
$_{8}$O	≤ 0.5	$_{23}$V	0.02	$_{47}$Ag	≤ 0.1
$_{9}$F	≤ 0.1	$_{24}$Cr	0.2	$_{50}$Sn	0.1
$_{11}$Na	0.6	$_{25}$Mn	0.1	$_{78}$Pt	<0.7

imply the vacancy-formation enthalpy to be equal in both states.

The measured S curves for 50- and 750-at. ppm carbon-doped iron show trapping of positrons in carbon-vacancy pairs below the Curie temperature. This will allow us to deduce information about the vacancy-formation enthalpy in the ferromagnetic state, provided that the presence of carbon-vacancy pairs is correctly accounted for in the analysis. This can be done by using a three-state trapping model (instead of the conventional two-state trapping model[26]), where the third annihilation state corresponds to the positron trapped in the carbon-vacancy pair. We will assume that the configuration of the carbon-vacancy pair is that calculated by Johnson and Damask[27]: The carbon atom is located on an interstitial octahedral positron adjacent to the vacancy and relaxes slightly into the latter, but remains in an off-center position. A very recent electronic tight-binding calculation, including a repulsive Born-Mayer potential, by Masuda confirmed this configuration[28]; there also exists experimental evidence supporting it.[5,21] It should be mentioned that only carbon atoms in interstitial solution are able to form stable carbon-vacancy pairs.[28] Therefore, the fraction of carbon atoms in interstitial solution at each temperature must be known to analyze the S curves in a three-state trapping model. This knowledge can be found partly in the phase diagram of the iron-carbon system and partly in the solubility curves of ϵ-carbide and cementite.[29,30] All the necessary tools to determine the vacancy-formation enthalpy in the ferromagnetic state by using the carbon-vacancy pair as an indirect probe are in principle available.

The experimental techniques applied to measure the S curve will be described in Sec. II. In Sec. III the measured S curves for the three types of iron (pure, 50-at. ppm carbon-doped, and 750-at. ppm carbon-doped) are presented and analyzed to determine the vacancy-formation enthalpy in both the ferromagnetic and paramagnetic state. In Sec. IV some implications are discussed. It will be shown that the ferromagnetic vacancy-migration enthalpy that is found by subtracting the vacancy-formation enthalpy in the ferromagnetic state from the recently reported activation enthalpy for self-diffusion in this state is now in agreement with the one-interstitial model. Some preliminary results of this work were already presented by De Schepper *et al.*[31]

II. EXPERIMENTAL

The very pure iron was prepared at the Centre d'Etudes Nucléaires de Grenoble, using conventional preparation techniques.[32] The complete chemical analysis of the final material is given in Table II. For the preparation of the carbon-doped samples the extremely pure iron was used; it was melted in an induction furnace filled with He gas in the presence of pure graphite. Carbon concentrations were measured either by internal-friction or by residual-resistivity—ratio measurements.

Cylindrically shaped samples with a central hole to contain the positron source were prepared (see Fig. 1). New degreased gimlets were used to drill the central hole. Before entering the ^{22}Na source, the specimens were chemically polished in a mixture of 6 vol. % HF, 25 vol. % H_2O_2, and 69 vol. % H_2O and carefully washed in pure ethanol to remove the heavily deformed surface layer. It has indeed been observed that the presence of this layer can given rise to trapping of positrons at dislocationlike defects in the temperature range where the vacancy concentration is still too low to be detected (this is the so-called prevacancy region).[33] The aqueous solution of the ^{22}Na source (~ 10 μCi) was injected in the central hole of the specimen. To avoid oxidation the water was evaporated quickly under a vacuum of $\sim 10^{-2}$ Torr in a crucible filled with P_2O_5; next the cylindrical specimens were closed by elec-

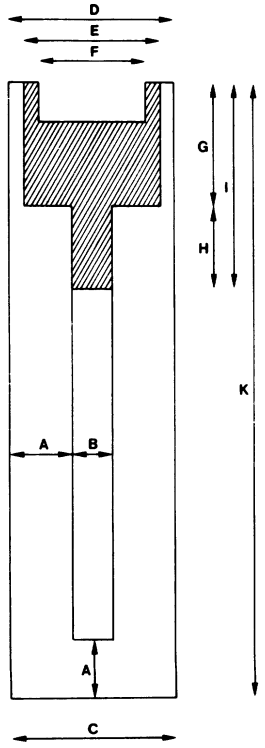

FIG. 1. Sealed source specimen for high-temperature positron annihilation experiments. $A=1.2$ mm, $B=1.6$ mm, $C=4.0$ mm, $D=4.0$ mm, $E=3.0$ mm, $F=2.0$ mm, $G=3.0$ mm, $H=2.0$ mm, $I=5.0$ mm, $K=15$ mm.

tron beam welding in vacuum ($\sim 10^{-5}$ Torr) at Euratom (Geel, Belgium). The speciments were heated in a small furnace mounted in a quartz tube under a vacuum of $\sim 10^{-6}$ Torr. The temperature was measured by means of a NiCr-Ni thermocouple, and the furnace was controlled by a Rockwell International AIM-65 (Advanced Interactive Monitor) microcomputer. For the very pure iron and the iron doped with 50 at. ppm carbon, the S parameter was measured between ~ 600 and 1183 K at constant temperature (stability better than 1 K), starting at 1183 K. Measurements were made with intervals of 10 K. The disadvantage of this measuring program was the long time required for stabilizing the temperature (~ 45 min). Therefore, an alternative method was used for the measurements on the 750-at. ppm carbon-doped sample: A linear heating program was used and the energy of the annihilation γ rays was continuously recorded. The S parameter S_i at temperature T_i was then calculated from the energy distribution for the annihilation γ rays recorded in the temperature interval (T_i-5 K, T_i+5 K). By using this method, measurements could be acquired much faster. In both measuring programs, an S parameter was calculated from an energy distribution consisting of about 1.2×10^6 annihilations.

The energy of the annihilation γ rays was measured with an Ortec hyperpure Ge detector with an efficiency of 18% coupled to an Ortec model-572 amplifier. Pile-up rejection was used. Energies below 470 keV were cut off by an Ortec model-44 biased amplifier, while pulses above 700 keV were blocked by an external inhibit circuit. Two-point stabilization was applied using the 477.6-keV signal of a ^{7}Be source and the 661.6-keV signal of a ^{137}Cs source.

The resolution of the detector was 1.15 keV at 514 keV at a total count rate of 10 kHz. The calibration was 0.0295 keV per channel. A Digital Equipment Corporation VAX11/780 computer was used to fit and subtract the background and to calculate the S parameter.

Since we were interested in comparing directly the S curves measured for the three types of iron, it was necessary to normalize the data. This is due to the fact that in the calculation of the S parameter from the energy distribution of the annihilation γ rays, an energy window centered around the 511-keV annihilation line must be defined.[34] We normalize the S curves for 50- and 750-at. ppm carbon-doped samples in such a way that their prevacancy region coincided with that of the very pure iron sample. In the prevacancy region one expects the temperature dependence of the S parameter to be linear, provided that no prevacancy effects are observed. So we define the normalized S parameter S' by

$$S'=\left[S-b+\frac{ab'}{a'}\right]\frac{a'}{a}\ , \tag{1}$$

where S is the measured S parameter, $S'=a'T+b'$ is the equation of the straight line fitted to the prevacancy region of the very pure iron sample, and $S=aT+b$ is the equation of the straight line fitted to the prevacancy region of the 50-at. ppm or 750-at. ppm carbon-doped sample.

III. RESULTS AND ANALYSIS

A. Very pure iron

In Fig. 2 the measured S curve for the very pure iron sample is shown by dots. It is clear that , as mentioned in Sec. I, the effect of trapping of positrons in defects becomes observable in the neighborhood of the Curie temperature (1043 K).

In the analysis of this S curve, we will assume that the residual carbon concentration in the sample is sufficiently low to allow neglect of the influence of carbon-vacancy pairs. It will be shown at the end of this section that this assumption is justified. From Table II it can be seen that the residual carbon concentration in the very pure iron sample is less than or equal to 1 at. ppm.

Neglecting carbon-vacancy pairs, we can use the two-state trapping model and write for the temperature dependence of the S parameter[26];

$$S=\frac{S_{f,0}(1+\alpha T)+S_v A_v \exp(-H_f^v/kT)}{1+A_v\exp(-H_f^v/kT)}\ , \tag{2}$$

where

$$A_v=\lambda_f^{-1}\mu\exp(S_f^v/k)\ , \tag{3}$$

$S_{f,0}$ is the bulk S parameter at $T=0$ K, α is a constant describing the effect of thermal expansion, T is the temperature, S_v is the characteristic S parameter corresponding to annihilation of the positron in the vacancy, H_f^v is the vacancy-formation enthalpy, k the Boltzmann constant, λ_f is the bulk positron annihilation rate, μ the trapping rate of the positron in the vacancy, and S_f^v the vacancy-formation entropy. A_v is usually called the preexponential factor. By fitting a straight line to the prevacancy region in Fig. 2, we find that $S_{f,0}=0.5070$ and $\alpha=3.055\times 10^{-5}$ K^{-1}. The parameter S_v cannot be determined directly, since for α-iron there exists no temperature range where saturation of positron trapping in vacancies occurs. Some authors have solved this problem by taking for S_v the value corresponding to the observed saturation trapping in the δ phase[15,23]; this, however, requires measurements very close to the melting point (1809 K), and even

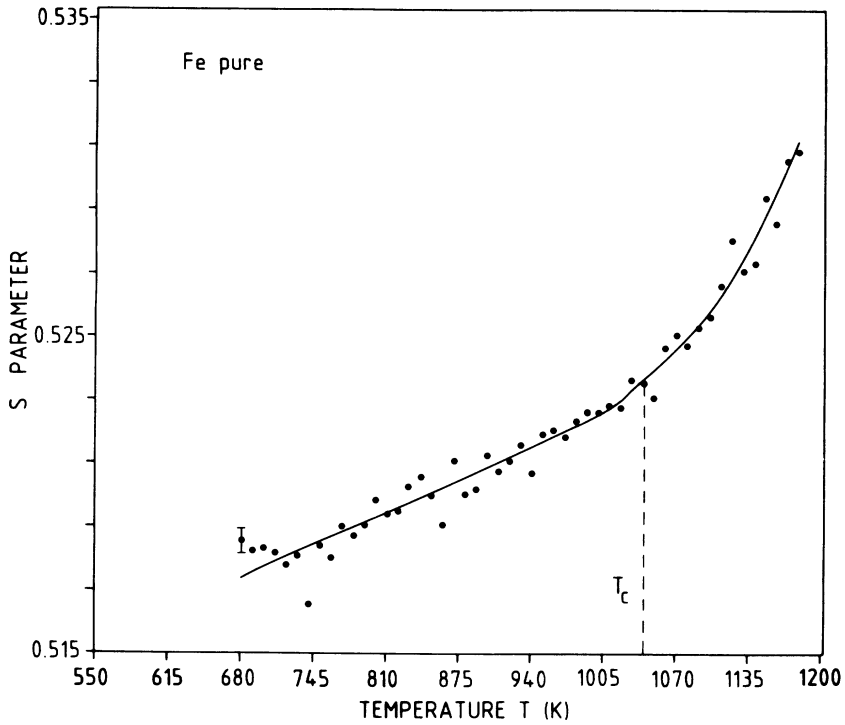

FIG. 2. Measured S curve for very pure α-iron (dots). The solid line is the calculated curve in the two-state trapping model ($S_v=0.595$, $A_v=4\times10^6$, $H^v_{f,p}=1.79$ eV, $H^v_{f,f}=2.0$ eV, $S_{f,0}=0.5070$, and $\alpha=3.055\times10^{-5}$ K^{-1}).

there it is not clear whether saturation of trapping is complete (see Fig. 4 in Ref. 23). Therefore, we preferred to fit the parameter S_v (together with A_v and H^v_f) to the experimental curve; this method was also used by Kim and Buyers.[24]

It was already mentioned in Sec. I that the vacancy-formation enthalpies in the ferromagnetic and paramagnetic state are not necessarily equal, although no discontinuity at the Curie point is observed in the S curve of Fig. 2. It has indeed been shown that the vacancy-formation enthalpy in a ferromagnetic material is temperature dependent, and given by[35]

$$H^v_f(T)=H^v_{f,p} \quad \text{if } R(T)=0\,,$$

and (4)

$$H^v_f(T)=(H^v_{f,f}-H^v_{f,p})R^2(T)+H^v_{f,p} \quad \text{if } R(T)\neq0$$

where $H^v_{f,p}$ is the temperature-independent value in the paramagnetic state, $H^v_{f,f}$ the temperature-independent value in the completely ordered ferromagnetic state (i.e., below $\sim0.4T_C$), and $R(T)$ is the so-called reduced spontaneous (or saturation) magnetization which is a characteristic for the degree of ferromagnetic order. The curve $R(T)$ is shown in Fig. 3. Since the theoretically calculated curve deviates somewhat from the experimental one, only the latter will be used in the calculations in this section. From Fig. 3 and Eq. (4), it can be concluded that $H^v_f(T)$ changes in a continuous way when passing the Curie temperature T_C if the paramagnetic value $H^v_{f,p}$ is not equal to the value in the completely ordered ferromagnetic state [i.e., $R(T)=1$] $H^v_{f,f}$. So it is not true that a discontinuity should be observed at the Curie point when $H^v_{f,p}$ is not equal

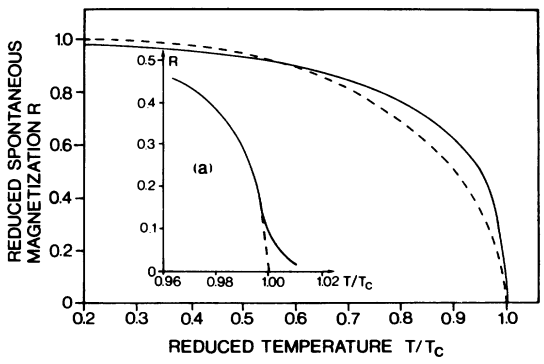

FIG. 3. Temperature dependence of the reduced spontaneous magnetization R for α-iron after Potter (Ref. 36) (solid line). The dashed line represents the calculated temperature dependence based on the Brillouin function for spin $\frac{1}{2}$.

to $H^v_{f,f}$, as was argued by Kim and Buyers[24] to justify the assumption that $H^v_{f,p}=H^v_{f,f}$. It can also be seen from Fig. 3 that in the paramagnetic temperature range just above T_C some ordering still exists, which is presumably due to short-range spin order.[36,37]

By substituting Eq. (4) into (2), we end up with four parameters to be fitted simultaneously to the experimental curve of Fig. 2, i.e., A_v, S_v, $H^v_{f,p}$, and $H^v_{f,f}$. By using a general minimization program based on the so-called Marquardt algorithm,[38] the following results were obtained:

(1) For the parameter $H^v_{f,p}$, it was found that

$$H^v_{f,p}=1.79\pm0.10 \text{ eV} .$$

This value is rather insensitive to variations of the other parameters within the range indicated below.

(2) The simultaneous fitting of A_v and S_v to the experimental curve is a rather difficult task since S_f only appears in the preexponential product A_vS_v in the numerator of Eq. (2). The difficulties involved are discussed in Appendix A, but they are not relevant to the present discussion, since the vacancy-formation enthalpies $H^v_{f,f}$ and $H^v_{f,p}$ are rather insensitive to the uncertainties in A_v and S_v. A good fit to the experimental curve is obtained for

$$A_v=(4\pm1)\times10^6$$

and

$$S_v=0.595\pm0.008 .$$

(3) The parameter $H^v_{f,f}$ could not be determined with any reasonable accuracy. This can be understood by the fact that no trapping in defects is observed in the S curve of Fig. 2; therefore, one cannot expect to find any information about defects in this temperature range. It can, however, be concluded that $H^v_{f,f}\geq H^v_{f,p}$, because otherwise the effect of positron trapping in defects would be observed below the Curie temperature.

The value for the vacancy-formation enthalpy cited above is higher than the values published so far (see Table I). In our opinion this is due to the fact that the iron sample used in the present experiment has the lowest level of residual carbon (see Table II). It will indeed be shown further in this section that a two-state trapping model can only be used in the analysis of the S curve if the residual carbon concentration in the sample is in the order of 1 at. ppm. If the carbon content of the sample is higher, it is no longer a good approximation to neglect the influence of carbon-vacancy pairs and, consequently, application of a two-state trapping model will lead to an underestimation of the value of the vacancy-formation enthalpy.

The solid line in Fig. 2 shows the calculated S curve using Eqs. (2)—(4), the experimental $R(T)$ values of Fig. 3, and the values of S_v, A_v, and $H^v_{f,p}$ given above. For reasons that will become clear later on in this section, the value of $H^v_{f,f}$ was chosen to be 2.0 eV. The fact that $H^v_{f,f}\neq H^v_{f,p}$ causes a small kink in the calculated curve near the Curie point but not a discontinuity.

B. 50-at. ppm carbon-doped iron

In Fig. 4 the measured (and normalized) S curve for 50-at. ppm carbon-doped iron is shown by dots. By comparing this curve with the curve for very pure iron (Fig. 2), it can be seen that the effect of positron trapping in defects may be observed, in the case of 50-at. ppm carbon-doped iron, at temperatures below the Curie point, and that, roughly speaking, the transition between the two regimes is less sudden. Therefore, it is clear that a three-state trapping model should be used in the analysis of the curve, the third annihilation state being the positron trapped in the carbon-vacancy pair. This is in agreement with earlier calculations of some of the present authors.[20] Nevertheless, it may be instructive to mention the results of an attempt which we have made to analyze the curve of Fig. 4 in the simple two-state trapping model. Using the same method as in the case of very pure iron, we could not find a close fit to the experimental curve if the parameters S_v and A_v were kept the same as for the case of pure iron. By lowering S_v, we obtained the solution $H^v_{f,p}=1.60$ eV for $A_v=1\times10^6$ and $S_v=0.57$. Alternatively, by lowering A_v, we obtained $H^v_{f,p}=1.53$ for $A_v=3\times10^5$ and $S_v=0.60$. In both cases the $H^v_{f,f}$ values were higher than, or equal to, the cited paramagnetic values. Although the physical relevance of these solutions is low, it is very interesting to note that in both cases considerably lower values for $H^v_{f,p}$ are found than for the cases of very pure iron. This shows that neglect of the formation of carbon-vacancy pairs leads to an underestimation of the value of the vacancy-formation enthalpy.

We will now proceed by analyzing the curve of Fig. 4 in a three-state trapping model, including the carbon-vacancy pair as a localization site for the positron. By simply extending the conventional two-state trapping model[26] and taking into account the thermodynamic concentration of carbon-vacancy pairs,[20] we obtain, for the temperature dependence of the S parameter,

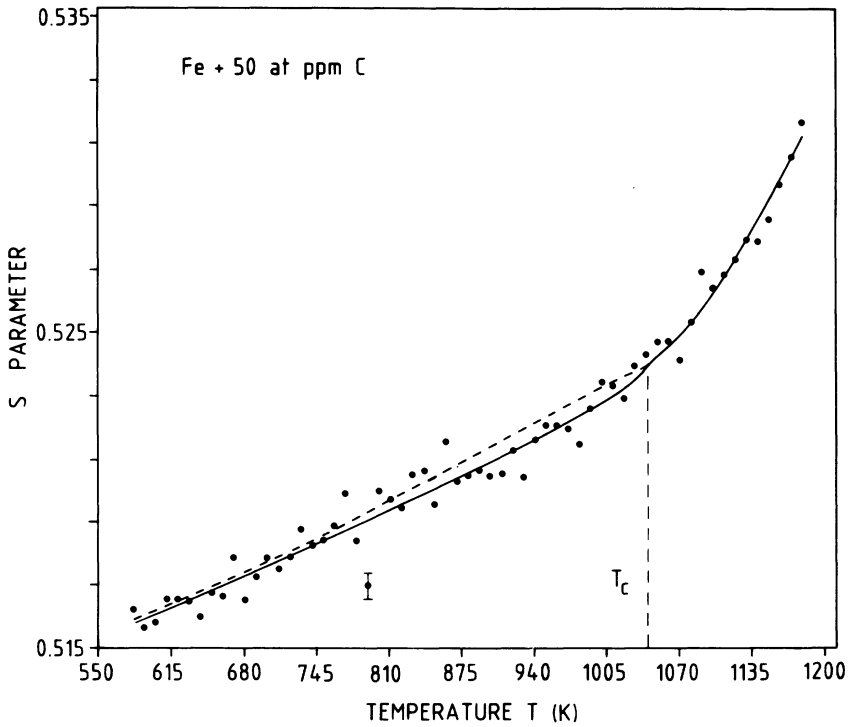

FIG. 4. Measured (normalized) S curve for 50-at. ppm carbon-doped α-iron (dots). The solid line is the calculated curve in the three-state trapping model for the parameters of Table III. The dashed line is the calculated curve for the same set of parameters, except $H^v_{f,f}=H^v_{f,p}=1.79$ eV.

$$S=\frac{S_{f,0}(1+\alpha T)+S_v(1-mc)A_v\exp(-H^v_f/kT)+S_p mcA_p\exp[-(H^v_f-E_B)/kT]}{1+(1-mc)A_v\exp(-H^v_f/kT)+mcA_p\exp[-(H^v_f-E_B)/kT]}\ , \tag{5}$$

where

$$A_p=\lambda_f^{-1}\mu'\exp(S^{vc}_f/k)\ , \tag{6}$$

m is a coordination number taken as 6,[20] c is the carbon concentration in interstitial solution, E_B is the binding energy of the carbon-vacancy pair, S_p is the characteristic S parameter associated with the vacancy pair, μ' the trapping rate for the positron in the vacancy pair, and S^{vc}_f the formation entropy of the vacancy pair.

The carbon concentration in interstitial solution, c, is temperature dependent, since the total carbon content of the sample cannot remain in interstitial solution in the complete temperature range of interest. In Fig. 5 the phase diagram for the iron-carbon system is shown, together with the solubility curves for cementite and ϵ-carbide. From the phase diagram, it can be seen that between 996 and 1183 K, the maximum concentration of carbon that can exist in solid solution in the ferrite matrix is given by the solvus line separating the two-phase area (austinite and ferrite) and the ferrite area. Approximating this solvus line by a straight line, we can write, for the maximum carbon concentration in solid solution, c,[39]

$$c=\{-1.107[T(\mathrm{K})-273]+1007.326\}\times10^{-6}$$
$$\text{for } 996\ \mathrm{K}\le T\le 1183\ \mathrm{K}\ . \tag{7}$$

Between 573 and 996 K the maximum concentration of carbon in solution is given by the solubility curve of cementite. According to Swartz,[40] the solubility of cementite under normal stress is given by

$$c=4.67\times10^{-2}\times10^{[0.31-2645/T(\mathrm{K})]}$$
$$\text{for } 573\ \mathrm{K}\le T\le 996\ \mathrm{K}\ . \tag{8}$$

These equations give the interstitial carbon concentration c to be used in Eq. (5) for those temperatures where the total carbon content of the sample is

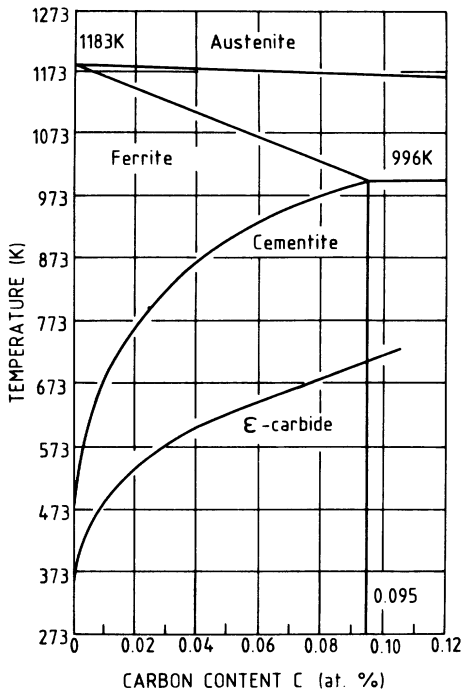

FIG. 5. Phase diagram of the iron-carbon system after Chipman (Ref. 39) together with the solubility curves for ϵ-carbide and cementite.

higher than the soluble content.

The vacancy-formation enthalpy H_f^v in Eq. (5) is again given by Eq. (4), with the experimental $R(T)$ values from Fig. 3. It should now be taken into account that, besides H_f^v, the parameter E_B is also dependent on the degree of ferromagnetic ordering. This can be seen in a recent electronic tight-binding—type calculation of the structure of the carbon-vacancy pair by Masuda.[28] It was calculated that the paramagnetic binding energy $E_{B,p}$ of the carbon-vacancy pair is about 0.5 eV.[28] This value was, however, based on a vacancy-formation enthalpy of about 1.3 eV, which is, in view of the results presented in this paper, too low. With the use of a vacancy-formation enthalpy of 1.8 eV, it was estimated that $E_{B,p}$ is about 0.65.[41] On the other hand, it was mentioned in Sec. I that the binding energy of the carbon-vacancy pair in the fully ordered ferromagnetic state $E_{B,f}$ is about 1.0 eV, if the vacancy-migration enthalpy of the one-interstitial model is applied.[20] If we assume the dependence of the binding energy on the degree of ferromagnetic ordering to be similar as that of the vacancy-formation enthalpy, we can write

$$E_B(T)=\begin{cases}E_{B,p} & \text{if } R(T)=0\\ (E_{B,f}-E_{B,p})R^2(T)+E_{B,p} & \text{if } R(T)\neq 0\end{cases}. \tag{9}$$

We will use further the values $E_{B,f}=1.0\pm0.1$ eV and $E_{B,p}=0.65\pm0.05$ eV. Equation (9) will be used to calculate the parameter E_B in Eq. (5).

The parameters S_v and A_v were already determined in the analysis of the S curve for very pure iron (Sec. III A). Since the S curve of Fig. 4 is normalized on the very pure iron curve, the parameters S_f and α also remain unchanged. We introduce, furthermore, the following approximations:

$$S_p \approx S_v \tag{10}$$

and

$$\mu \exp(S_f^v/k) \approx \mu' \exp(S_f^{vc}/k)\ . \tag{11}$$

The first approximation is justified by the fact that it has been observed that the lifetime of a positron trapped in a carbon-vacancy pair is 160 ps, which is almost equal to that in a single vacancy (175 ps).[5] The second approximation can be partly justified by the fact that the trapping rates of the carbon-vacancy pair and the vacancy are also comparable in magnitude.[7]

By using Eqs. (5)—(11) we can now fit the remaining parameter $H_{f,f}^v$ to the experimental curve of Fig. 4. This yields

$$H_{f,f}^v = 2.0\pm0.2$$

(in units of eV). The complete set of parameters is enumerated in Table III. The solid curve in Fig. 4 shows the S curve calculated with Eqs. (5)—(11) for the parameters of Table III. This curve fits well the experimental data in the paramagnetic state, where trapping mainly occurs in single vacancies, as well as in the ferromagnetic state where the observed deviation from the straight line of the prevacancy region (between $\sim$940 and 1043 K) is mainly due to trapping in carbon-vacancy pairs. Indeed, for very pure iron (Fig. 2), no significant trapping was observed in the ferromagnetic state. This was the reason why no value for $H_{f,f}^v$ could be found by analyzing the S curve for very pure iron; for 50-at. ppm carbon-doped iron, however, the small trap-

TABLE III. Numerical values used in the three-state trapping model calculations of S curves.

$A_v=A_p=(4\pm1)\times10^6$
$S_v=S_p=0.595\pm0.008$
$S_f=0.5070$
$\alpha=3.055\times10^{-5}$ K^{-1}
$m=6$
$E_{B,f}=1.0\pm0.1$ eV
$E_{B,p}=0.65\pm0.05$ eV
$H_{f,p}^v=1.79\pm0.10$ eV
$H_{f,f}^v=2.0\pm0.2$ eV

ping effect observed between ~940 and 1043 K allowed us to determine the value of $H^v_{f,f}$. The 10% uncertainty on the obtained $H^v_{f,f}$ value is mainly due to the uncertainty on the binding energy of the carbon-vacancy pair. Nevertheless, it is very unlikely that the vacancy-formation enthalpies in the ferromagnetic and paramagnetic states are equal. Indeed, the dotted line in Fig. 4 shows the calculated curve for the same parameters as were used to calculate the solid line (see Table III), except that now $H^v_{f,f}=H^v_{f,p}=1.79$ eV. It is clear that this assumption leads to an overestimation of the trapping due to carbon-vacancy pairs in the ferromagnetic state.

C. 750-at. ppm carbon-doped iron

In Fig. 6 the measured S curve for 750-at. ppm carbon-doped iron normalized on the prevacancy region of the very pure iron curve is shown by dots. The trapping effect in the ferromagnetic state is more pronounced than in the 50-at. ppm carbon-doped iron: A deviation from the prevacancy straight line already starts at ~875 K, reflecting considerable trapping in carbon-vacancy pairs between this temperature and ~1000 K. Above this temperature, the carbon content in interstitial solution in the ferrite matrix diminishes rapidly [see Fig. 5 and Eq. (7)], and consequently the equilibrium concentration of carbon-vacancy pairs is reduced correspondingly. Above the Curie temperature (1043 K), the effect of positron trapping in single vacancies is observed. The combination of both processes gives rise to the kink in the S curve between 1005 and 1043 K. Another interesting feature of the curve is that the $\alpha\rightarrow\gamma$ transition temperature (which for pure iron is 1183 K) is now observed between 1160 and 1170 K (the transition is reflected in the S curve by a strong and rather sharp reduction in the S parameter due to the lower bulk S parameter $S_{f,0}$ in the fcc structure[15,23–25]). This can also be understood on the basis of the phase diagram of the iron-carbon system (Fig. 5): For 750-at. ppm carbon content, the $\alpha\rightarrow\gamma$ transition temperature falls indeed about 15 K below the transition temperature for pure iron, as indicated by the A_3 line.

The solid line in Fig. 6 shows the calculated S curve in the three-state trapping model, using again the set of parameters enumerated in Table III. This curve fits very well the data points, in both the ferromagnetic and paramagnetic states. The position of the $\alpha\rightarrow\gamma$ transition is, of course, not correctly predicted, since only trapping in the ferrite matrix is

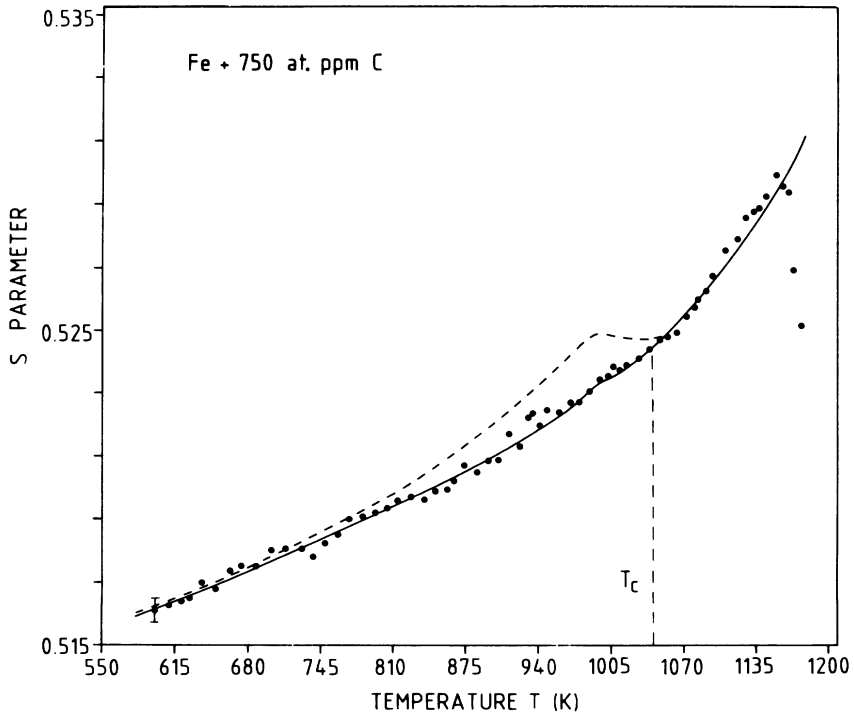

FIG. 6. Measured (normalized) S curve for 750-at. ppm carbon-doped α-iron (dots). The solid line is the calculated curve in the three-state trapping model for the parameters shown in Table III. The dashed line is the calculated curve for the same set of parameters, except that $H^v_{f,f}=H^v_{f,p}=1.79$ eV.

considered in the model.

An attempt was made to optimize some of the parameters of Table III (especially $H^v_{f,f}$), but no significant changes in the numerical values were found. The dotted line in Fig. 6 shows the curve calculated under the assumption that $H^v_{f,f}=H^v_{f,p}=1.79$ eV (other parameters remain the same as in Table III); as in the case of 50-at. ppm carbon-doped iron, this leads to a bad description of the ferromagnetic part of the S curve.

It seems that the solid curve underestimates slightly the amount of trapping of positrons in the paramagnetic state close to the $\alpha\rightarrow\gamma$ transition. This cannot be explained in the present model. It should be noted, however, that trapping of positrons at other sites than single vacancies and carbon-vacancy pairs in the ferrite matrix are not included. It could be suggested that between $\sim$1100 and $\sim$1160 K some positron trapping occurs at the interface between nucleating γ particles and the ferrite matrix. Also, a minor inaccuracy in Eq. (7) could be the reason for the deviation between the calculated curve and the measured one.

D. Very pure iron and the three-state trapping model

The three-state trapping model described in Sec. III B leads to very close agreement between the calculated curves for 50-at. ppm and 750-at. ppm carbon-doped iron and the experimental data if the parameters of Table III are used. In Sec. III A, we analyze the S curve for very pure iron in a two-state trapping model, assuming that the residual carbon content of about 1 at. ppm was sufficiently low to be neglected. If this assumption was valid, the experimental curve for very pure iron should also be well described by the three-state trapping model curve for a carbon content of 1 at. ppm. We calculated this curve (again for the set of parameters of Table III) and found that the difference with the solid line of Fig. 2 was so small that it was not representable on the scale of the figure. This justifies the assumption made in Sec. III A.

E. Comparison with other experiments

As can be seen from Table I, the paramagnetic vacancy-formation enthalpy found in this experiment is considerably higher than the enthalpies obtained in previous experiments.[15,23–25] In our opinion this is due to the fact that the residual interstitial impurity content of our pure iron is smaller than in the other cases; therefore, the contribution of interstitial impurity-vacancy pairs (especially carbon-vacancy pairs) to the measured line-shape parameters is the smallest (in fact, for carbon-vacancy pairs it can be neglected as shown in Sec. III D). It was indeed shown in Sec. III B that the analysis of the temperature dependence of a line-shape parameter measured on a sample containing 50 at. ppm carbon in the two-state trapping model (i.e., neglecting trapping in carbon-vacancy pairs) leads to a vacancy-formation enthalpy which is too low. A similar effect has most probably influenced the previously published formation enthalpies. For instance, the lowest enthalpy, 1.4 eV, was obtained by Kim and Buyers[24] by analyzing the peak counting rate (PCR) in angular correlation on an iron sample containing 110 wt. ppm oxygen, 12 wt. ppm nitrogen, and 10 wt. ppm carbon. When looking in detail at the temperature dependence of the PCR (Fig. 1 in Ref. 24), it can be seen that some trapping in the ferromagnetic state was observed. In our opinion this is due to interstitial-impurity–vacancy pairs. However, a two-state trapping model was used in the analysis (assuming the ferromagnetic and paramagnetic vacancy-formation enthalpies to be equal), leading to an underestimation of the vacancy-formation enthalpy.

IV. SOME IMPLICATIONS

The values for the vacancy-formation enthalpies in the paramagnetic and ferromagnetic states obtained in the preceding section (see Table III) can be combined with self-diffusion enthalpy values to obtain the vacancy-migration enthalpies. It is indeed known that the latter are found by subtracting the vacancy-formation enthalpy from the enthalpy for self-diffusion, provided that the latter process is caused by monovacancies.[42] There is so far no evidence on which to doubt this point in the temperature range of interest in α-iron.[18]

Recently some of the present authors analyzed existing self-diffusion data on iron and obtained, for the self-diffusion enthalpy in the paramagnetic state, $Q_{SD,p}=2.36$ eV,[19] in close agreement with the value given by Hettich *et al.*[18] Combining this value with the corresponding vacancy-formation enthalpy of Table III, we obtain, for the vacancy-migration enthalpy in the paramagnetic state, $H^v_{m,p}=0.6\pm0.1$ eV. This value is lower than accepted so far.[23] For the value $H^v_{m,f}$ in the ferromagnetic state we can only give a rather broad range: $0.16\ \text{eV}\leq H^v_{m,f}\leq 0.95$ eV.

The lower limit arises from the fact that $Q_{SD,f}$ is in any case higher than $Q_{SD,p}$, and the upper limit from the fact that $Q_{SD,f}\leq 2.75$ eV.[19] This $Q_{SD,f}$ value is considerably lower than the original one obtained by Hettich *et al.*,[18] which was about 3.0 eV. In Ref. 19 it is, however, clearly shown that this value is most probably overestimated. The result for

$H^v_{m,f}$ cited above is definitely in favor of the one-interstitial model. This overrules the main remaining argument against this model.[15,17]

These experiments also confirm the main properties of the carbon-vacancy pair, i.e., the high binding energy (see Table III) and the off-center position of the carbon atom. These properties have been predicted theoretically,[27,28] and confirmed earlier by positron lifetime measurements[4,5] at ambient temperatures. Furthermore, it has been shown that the trapping rate of positrons into carbon-vacancy pairs present in thermodynamical equilibrium with single vacancies must be high, i.e., of the same order of magnitude as the trapping rate into stable carbon-vacancy pairs and single vacancies.

Finally, by comparing the values for the activation enthalpy for vacancy formation in the paramagnetic and ferromagnetic states (see Table III), it can be concluded that the ferromagnetic contribution to the enthalpy is rather high, probably of the order of 0.2 eV. This contribution is higher than the estimate obtained by the simple nearest-neighbor spin-exchange model.[37] The latter model yields a ferromagnetic contribution of $\sim$0.07 eV, as mentioned by Schaefer *et al.*[15] (Table I). The nearest-neighbor spin-exchange model contains, however, some major approximations of which the validity can be questioned: (a) only nearest-neighbor spin interaction occurs in the perfect lattice, (b) when forming a vacancy only nearest-neighbor bonds are broken and the other bonds remain unaffected, and (c) no magnetostrictive effects occur when forming a vacancy. The approximation (a) is not in agreement with elastic constant measurements by Dever[43] who concluded that second-nearest-neighbor spin interaction is the dominant process; this also makes assumption (b) questionable. Also, no evidence can be given to support approximation (c); in fact, magnetostrictive effects have been suggested to explain the ferromagnetic self-diffusion anomaly.[44]

V. SUMMARY AND CONCLUSIONS

Positron annihilation S-parameter measurements on pure and carbon-doped (50 and 750 at. ppm) α-iron in thermal equilibrium have shown that trapping in both monovacancies and carbon-vacancy pairs occurs. For the case of very pure iron, trapping of positrons in carbon-vacancy pairs could, however, be neglected; by using the conventional two-state trapping model, it was concluded that the paramagnetic vacancy-formation enthalpy is 1.79 ± 0.10 eV. No value could be deduced for the ferromagnetic state since no significant trapping was observed below the Curie point.

In contrast, the S curve of 50-at. ppm carbon-doped α-iron showed trapping in carbon-vacancy pairs below the Curie point. By using a three-state trapping model, where the third state corresponds to the positron trapped in the carbon-vacancy pair, it was found that the ferromagnetic vacancy-formation enthalpy is 2.0 ± 0.2 eV. So the carbon-vacancy pair could be used as a probe to determine this parameter. Furthermore, the calculated S curve for 750-at. ppm carbon-doped α-iron in the three-state trapping model, using the cited vacancy-formation enthalpy values, was in very close agreement with the experimental curve.

The present experiments confirm the main properties of the carbon-vacancy pair, i.e., the high binding energy and the off-center position of the carbon atom. It was shown that these pairs are highly effective in trapping positrons, even in thermal equilibrium above their dissociation temperature. By combining the obtained vacancy-formation enthalpy values with recently published self-diffusion enthalpy data on α-iron, the applicability of the one-interstitial model is confirmed for this metal.

ACKNOWLEDGMENTS

The authors express their gratitude to Dr. J. Van Audenhove and Dr. E. Freistedt of EURATOM (Belgium) for electron beam welding of the specimens. Helpful discussions with Professor P. Hautojärvi, Dr. A. Vehanen, Dr. K. Masuda, and Dr. P. Lucasson are highly appreciated. Thanks are due to Dr. A. Keupers for writing the minimization computer program. Financial support of the Belgian science supporting institute (Interuniversitair Instituut voor Kernwetenschappen) is acknowledged.

APPENDIX A: DETERMINATION OF A_v AND S_v

The main reason for the difficulties encountered in the simultaneous fitting of A_v and S_v to the experimental curve is that S_v (which is about 6 orders of magnitude smaller than A_v) only appears in the product A_vS_v in the numerator of Eq. (2).

Fortunately we could take advantage of the fact that A_v values for the other bcc metals have been determined[45]: A_v is 1×10^6 for V and Nb, 2×10^6 for Ta and Mo, and 4×10^6 for W. Therefore, we fixed A_v for bcc iron between 9×10^5 and 5×10^6. It should be noted that all the previously reported A_v values for α-iron (see Table IV) fall within this range, except for the extremely low value, compared to the other bcc metals, obtained by Kim and Buyers.[24]

Despite this rather small range defined for A_v, two equally good fits were obtained for the follow-

ing sets of parameters: (i) $H^v_{f,p}=1.76\pm0.10$ eV, $A_v=(2\pm1)\times10^6$, $S_v=0.624\pm0.008$, and (ii) $H^v_{f,p}=1.79\pm0.10$ eV, $A_v=(4\pm1)\times10^6$, $S_v=0.595\pm0.008$.

The A_v value of set (i) is very close to previously reported values for α-iron (Table IV). The corresponding $S_v/S_{f,0}$ ratio is about 1.23 since $S_{f,0}=0.5070$ (see Sec. IV A), which seems to be rather high compared to the ratios $F_v/F_{f,0}$ listed in Table IV. It is indeed known that the ratio $F_v/F_{f,0}$ is, for instance, in general higher for normalized peak counting rates than for S parameters[46]; therefore, the $S_v/S_{f,0}$ ratio of set (i) is rather high compared to the result obtained by Matter *et al.*[23] To our knowledge there exists in the literature only one other S-parameter experiment in thermal equilibrium on iron[47], which was not, however, analyzed in the trapping model. If we assume that complete saturation of trapping in vacancies was observed near the melting point (see Fig. 2 in Ref. 47), then we obtain $S_v/S_{f,0}\approx1.18$; if saturation was not complete this ratio would be slightly higher. Also, this result seems to indicate that the value $S_v/S_{f,0}$ of set (i) is too high.

For set (ii) the A_v value is somewhat higher than the previously reported values for bcc iron (Table IV); nevertheless, it falls within the range of the other bcc metals indicated above. On the other hand, the corresponding $S_v/S_{f,0}$ ratio (equal to 1.18) is in excellent agreement with the value which we derived from the S curve measured by Schulte *et al.*[47] It is also a reasonable number compared to the $F_v/F_{f,0}$ ratios listed in Table IV.

Therefore, we prefered to use the set of parameters (ii) in Sec. III. It should be stressed, however, that when repeating the analysis described in Sec. III for the set (i) no significant difference on $H^v_{f,f}$ was found. We also recalculated the S curves of Figs. 2, 4, and 6 for set (i), but the differences were also negligible. So we can conclude that the uncertainties in the determination of A_v and S_v are not relevant to the fitting of $H^v_{f,p}$ and $H^v_{f,f}$ to experimental curves.

TABLE IV. Values for the preexponential factor A_v and the parameter $F_v/F_{f,0}$ used in the two-state trapping-model analysis of the temperature dependence of a characteristic annihilation parameter F for α-iron in thermal equilibrium.

A_v	$F_v/F_{f,0}$	Method[a]	Reference
$(2\pm1)\times10^6$	1.25	NPC	23
3×10^5	1.152	NPC	24
1×10^6	$\frac{1}{1.177}$	W	15
1×10^6	?	W	25
$(4\pm1)\times10^6$	1.18	S	this work

[a]NPC is the normalized peak counting rate in angular correlation, W is the Wing parameter in Doppler broadening, S is the S parameter in Doppler broadening.

[1]L. J. Cuddy, Acta Metall. 16, 23 (1968).

[2]J. Nihoul, in *Vacancies and Interstitials in Metals,* edited by A. Seeger, D. Schumacher, W. Schilling, and J. Diehl (North-Holland, Amsterdam, 1970), p. 839.

[3]L. De Schepper, J. Cornelis, G. Knuyt, J. Nihoul, and L. Stals, Phys. Status Solidi A 61, 341 (1980).

[4]P. Hautojärvi, T. Judin, A. Vehanen, J. Yli-Kauppila, J. Johansson, J. Verdone, and P. Moser, Solid State Commun. 29, 855 (1979).

[5]P. Hautojärvi, J. Johansson, A. Vehanen, J. Yli-Kauppila, and P. Moser, Phys. Rev. Lett. 44, 1326 (1980).

[6]S. Tanigawa, K. Hinode, N. Owada, M. Doyama, and S. Okuda, in *Proceedings of the Vth International Conference on Positron Annihilation,* edited by R. R. Hasiguti and K. Fujiwara (The Japan Institute of Metals, Sendai, 1979), p. 501.

[7]A. Vehanen, P. Hautojärvi, J. Johansson, J. Yli-Kauppila, and P, Moser, Phys. Rev. B 25, 762 (1982).

[8]W. Frank and A. Seeger, Radiat. Eff. 55, 111 (1981).

[9]P. Hautojärvi and A. Vehanen, Radiat. Eff. Lett. 58, 77 (1981).

[10]J. Verdone, P. Moser, W. Chambron, P. Hautojärvi, J. Johansson, and A. Vehanen, J. Magn. Magn. Mater. 19, 296 (1980).

[11]M. Kiritani, in *Proceedings of the Yamada Conference V on Point Defects and Defect Interactions in Metals,* edited by J. Tahamura (University of Tokyo Press, Tokyo, 1982), p. 508.

[12]E. Kuramoto, N. Yoshida, and K. Kitajima, in *Proceedings of the Yamada Conference V on Point Defects and Defect Interations in Metals,* Ref. 11.

[13]T. Tabata, H. Fujita, H. Ishii, K. Igaki, and M. Isshiki, Scr. Metall. 14, 1317 (1977).

[14]J. Verdone, A. Bourret, and P. Moser, Radiat. Eff. 61, 99 (1982).

[15]H. E. Schaefer, K. Maier, M. Weller, D. Herlach, A. Seeger, and J. Diehl, Scr. Metall. 11, 803 (1977).

[16]W. Decker, J. Diehl, A. Dunlop, W. Frank, H. Kronmüller, W. Mensch, H. E. Schaefer, B. Schwendemann, A. Seeger, H. P. Stark, F. Walz, and M. Weller, Phys. Status Solidi A 52, 239 (1979).

[17]W. Frank, in *Proceedings of the Yamada Conference V on Point Defects and Defect Interactions in Metals,* Ref. 11.

[18]G. Hettich, H. Mehrer, and K. Maier, Scr. Metall. 11, 795 (1977).

[19]L. De Schepper, G. Knuyt, and L. M. Stals, J. Phys.

Chem. Solids 44, 171 (1983).
[20]L. De Schepper, G. Knuyt, and L. M. Stals, Phys. Status Solidi A 67, 153 (1981).
[21]M. Weller, J. Diehl, and W. Mensch, Phys. Status Solidi A 60, 93 (1980).
[22]H. Takahashi, T. Takeyama, S. Nakahigashi, and M. Terasawa, J. Nucl. Mater. 98, 227 (1981).
[23]H. Matter, J. Winter, and W. Triftshäuser, Appl. Phys. 20, 135 (1979).
[24]S. Kim and W. Buyers, J. Phys. F 8, L103 (1978).
[25]K. Maier, H. Metz, D. Herlach, and H. E. Schaefer, J. Nucl. Mater. 69-70, 589 (1978).
[26]D. Bergerson and M. J. Stott, Solid State Commun. 7, 1203 (1969); D. C. Connors and R. N. West, Phys. Lett. 30A, 24 (1969).
[27]R. A. Johnson and A. C. Damask, Acta Metall. 12, 443 (1964).
[28]K. Masuda, in *Proceedings of the Yamada Conference V on Point Defects and Defect Interactions in Metals,* Ref. 11.
[29]J. Chipman, Metall. Trans. 3, 5 (1972).
[30]J. C. Swartz, Trans. AIME 239, 68 (1967).
[31]L. De Schepper, D. Segers, G. Knuyt, J. Van Oppen, J. Dorikens-Vanpraet, M. Dorikens, L. M. Stals, and P. Moser, in *Proceedings of the Yamada Conference V on Point Defects and Defect Interactions in Metals,* Ref. 11.
[32]F. Vanoni, Ph.D. thesis, University of Grenoble, 1973 (unpublished).
[33]D. Segers, L. De Schepper, L. Dorikens-Vanpraet, M. Dorikens, G. Knuyt, L. Stals, and P. Moser, Phys. Lett. 89A, 347 (1982).
[34]I. K. MacKenzie, J. A. Eady, and R. Gingerich, Phys. Lett. 33A, 279 (1970).
[35]M. Schoijet and L. A. Girifalco, J. Phys. Chem. Solids 29, 481 (1968).
[36]H. H. Potter, Proc. R. Soc. London Ser. A 146, 362 (1934).
[37]L. Ruch, D. R. Sain, H. L. Yeh, and L. A. Girifalco, J. Phys. Chem. Solids 37, 649 (1976).
[38]D. W. Marquardt, J. Soc. Ind. Appl. Math. 11, 431 (1963).
[39]J. Chipman, Metall. Trans. 3, 5 (1972).
[40]J. C. Swartz, Trans. AIME 239, 68 (1967).
[41]K. Masuda (private communication).
[42]A. C. Damask and G. Dienes, *Point Defects in Metals* (Gordon and Breach, New York, 1963).
[43]D. J. Dever, J. Appl. Phys. 43, 3293 (1972).
[44]R. T. Borg and C. E. Birchenall, Trans. Metall. Soc. AIME 218, 980 (1960).
[45]K. Maier, M. Peo, B. Saile, H. E. Schaefer, and A. Seeger, Philos. Mag. A 40, 701 (1979).
[46]This can be seen by comparing Fig. 3.2. in *Positrons in Solids,* edited by Hautojärvi (Springer, Berlin, 1979), p. 99, and Fig. 1 in the paper by B. T. A. McKee, W. Triftshäuser, and A. T. Stewart, Phys. Rev. Lett. 28, 358 (1972).
[47]C. W. Schulte, J. L. Campbell, and J. A. Jackman, Appl. Phys. 16, 29 (1978).